

NO-A192 103

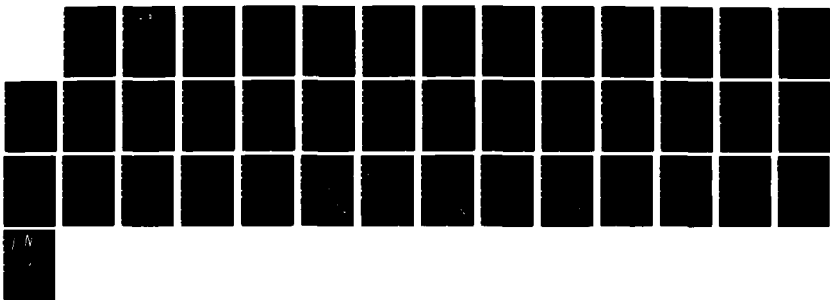
SPECTROSCOPY AND ENERGY TRANSFER KINETICS OF THE
INTERHALOGENS(U) ILLINOIS INST OF TECH CHICAGO
M C HEAVEN 08 FEB 88 AFOSR-TR-88-0128 AFOSR-85-0210

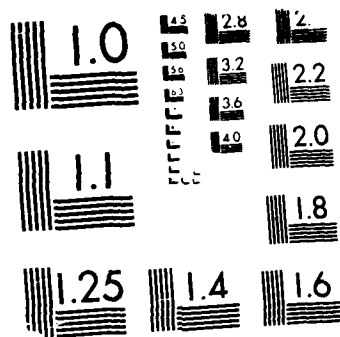
171

UNCLASSIFIED

F/G 7/2

NL





MICROCOPY RESOLUTION TEST CHART
 1000

AD-A192 103

REPORT DOCUMENTATION PAGE

ELECTE

MAR 01 1988

1b. RESTRICTIVE MARKINGS

2a. SECURITY CLASSIFICATION AUTHORITY

3. DISTRIBUTION/AVAILABILITY OF REPORT

2b. DECLASSIFICATION/DOWNGRADING SCHEDULE

Approved for public release:
Distribution unlimited.

4. PERFORMING ORGANIZATION REPORT NUMBER

5. MONITORING ORGANIZATION REPORT NUMBER(S)

AFOSR-TR-88-0128

6a. NAME OF PERFORMING ORGANIZATION
Illinois Institute of
Technology6b. OFFICE SYMBOL
(If applicable)

7a. NAME OF MONITORING ORGANIZATION

AFOSR/NC

6c. ADDRESS (City, State and ZIP Code)
3300 South Federal Street
Chicago, IL 606167b. ADDRESS (City, State and ZIP Code)
Building 410
Bolling AFB, DC 20332-64488a. NAME OF FUNDING/SPONSORING
ORGANIZATION
AFOSR8b. OFFICE SYMBOL
(If applicable)
NC

9. PROCUREMENT INSTRUMENT IDENTIFICATION NUMBER

AFOSR - 85 - 0210

8c. ADDRESS (City, State and ZIP Code)
Building 410
Bolling AFB, DC 20332-6448

10. SOURCE OF FUNDING NOS.

PROGRAM
ELEMENT NO.PROJECT
NO.TASK
NO.WORK UNIT
NO.11. TITLE (Include Security Classification) Spectroscopy and
Energy Transfer Kinetics of the Interhalogens

61102F

2303

B1

12. PERSONAL AUTHOR(S)

Michael C. Heaven

13a. TYPE OF REPORT

Final

13b. TIME COVERED

FROM 6/18/85 TO 11/14/87

14. DATE OF REPORT (Yr., Mo., Day)

02/08/88

15. PAGE COUNT

40

16. SUPPLEMENTARY NOTATION

17. COSATI CODES

FIELD GROUP SUB. GR.

18. SUBJECT TERMS (Continue on reverse if necessary and identify by block number)

Chemical Lasers

Halogens

Metastable States

Interhalogens

Energy Transfer

Singlet Oxygen

19. ABSTRACT (Continue on reverse if necessary and identify by block number)

The electronic spectra and energy transfer pathways of matrix isolated IF and I_2 have been investigated. Laser excitation of matrix isolated IF revealed the presence of three electronic states which had not been observed previously. The lowest energy state was identified as $A^{1/2} \Pi(2)$. Determination of the position and lifetime of this state has provided a means for assessing its role in the chemical excitation of the 3 state. The higher energy states have been tentatively assigned to a doubly excited electronic configuration.

Continued on back.

20. DISTRIBUTION AVAILABILITY OF ABSTRACT

UNCLASSIFIED UNLIMITED ☒ SAME AS RPT ☐ DTIC USERS ☐

21. ABSTRACT SECURITY CLASSIFICATION

UNCLASSIFIED

22a. NAME OF RESPONSIBLE INDIVIDUAL

Dr Francis J. Wodarczyk

22b. TELEPHONE NUMBER

(Include Area Code)
(202) 767-4963

22c. OFFICE SYMBOL

NC

The I_2 A-X system was studied in Ar, Kr, and Xe matrices. Analyses of the emission spectra showed that previous vibrational assignments were in error. The A state lifetime was found to be $50 \pm 15 \mu s$ in all three matrix hosts. Polarization measurements and excitation spectra showed that the A state was populated via the A+X and $^1\Pi(1u)+X$ transitions.

Emission from I^* atoms was observed at low iodine:rare gas dilution ratios. Excitation spectra, recorded by monitoring the atomic emission intensity as a function of laser wavelength, were identical to those observed for the I_2 A-X system. Thus, the atoms were excited by energy transfer from $I_2(A)$. Electronic energy transfer was also noted in matrices which contained iodine co-deposited with oxygen. Excitation of $I_2(A)$ resulted in emission from the O_2 a-X system. Both of these energy transfer processes are of relevance to the chemically pumped oxygen-iodine laser.

The radiative lifetime of ClF(B) was measured in the gas-phase. After correction for the effects of a strongly fluorescent contaminant, the lifetime was found to be $300 \pm 50 \mu s$. This corresponds to an electronic transition dipole of $1 \text{ Rel} = 0.1 \pm 0.014 \text{ D}$. The rate for self-quenching was found to be $2.3 \times 10^{-11} \text{ cm}^3 \text{ molecule}^{-1} \text{ s}^{-1}$. Preliminary calculations indicate that lasing of the ClF B-X transition can be achieved by optical pumping.

Continuous wave excitation and wavelength-resolved fluorescence techniques were used to study the self-quenching and energy transfer kinetics of $Br_2(B)$. A self-quenching rate constant of $4 \times 10^{-10} \text{ cm}^3 \text{ molecule}^{-1} \text{ s}^{-1}$ was observed for the levels with $v' > 10$, $J' > 15$, in excellent agreement with the results from pulsed measurements. The rate constant for rotational energy transfer (summed over all final states) was found to be $\approx 6 \times 10^{-11} \text{ cm}^3 \text{ molecule}^{-1} \text{ s}^{-1}$. An upper bound of $5 \times 10^{-12} \text{ cm}^3 \text{ molecule}^{-1} \text{ s}^{-1}$ was established for the vibrational transfer rate constant. These results are at variance with the energy transfer rate constants obtained from models of the time-resolved fluorescence decay kinetics.

(I.) Observation of New Low-Lying Electronic States of Iodine Monofluoride

Laser excitation techniques were used to study IF isolated in a solid Ar matrix. Excitation and emission spectra of the B-X system indicated that the valence states of IF were not strongly perturbed by the matrix environment. The fluorescence decay lifetime of the B state showed no evidence of matrix induced non-radiative decay channels.

Excitation of IF at wavelengths greater than 535 nm produced a long-lived emission in the far-red spectral region. From an analysis of the time and wavelength resolved fluorescence it was found that $A' \ ^3\Pi(2)$ was the emitting state. Determination of T_e for the A' state was used to show that participation of this state in the $O_2^1\Delta_g$ excitation of the B state was energetically feasible.

Short wavelength ($\lambda < 474$ nm) excitation of IF resulted in a far-red emission system that originated from a previously unobserved electronic state (α). Vibrational analysis established that the transition terminated on the ground state, and that the α state lies approximately 330 cm^{-1} above the B state. The strongly forbidden α -X system radiates with a 5 ms lifetime.

Absorption spectra, recorded by monitoring the $\alpha \rightarrow X$ emission while scanning the laser wavelength, revealed the presence of another new electronic state (β). The β -X intensity distribution and vibrational spacing of the excited state indicate that β is slightly more strongly bound than the B state. Rapid energy transfer from β to α precludes the detection of emission from β . This transfer is facilitated by a large Franck-Condon overlap between β , $v'=0$ and the repulsive limb of the α state.

Qualitative electronic structure arguments have been advanced for tentative assignment of α to $2422\text{ }^1\Delta(2)$ and β to $2422\text{ }^3\Sigma^-(1)$. This work has been described in detail in reference 1.

Approved for public release,
distribution unlimited

88 2 _ 26 03

(II.) The Spectroscopy and Dynamics of Matrix Isolated Iodine

Some methods used to prepare samples of matrix isolated IF resulted in the concurrent trapping of I_2 . Consequently, in the process of studying IF a number of interesting aspects of the behavior of matrix isolated I_2 were noted. As these properties were of relevance to the chemically pumped oxygen-iodine laser (COIL) they were investigated in some detail.

These studies were conducted in Ar, Kr, and Xe matrices. Gas mixtures of I_2 in a rare gas host were deposited on a copper disk which was held at temperatures between 10 and 20 K. Dilution ratios (I_2 : rare gas) in the range of 1:1000 to 1:300 were used. The samples were excited by the pulses from a tunable dye laser, or the second harmonic (532 nm) from a Nd/YAG laser. The laser induced fluorescence was dispersed by a 0.25m monochromator. Light in the 400-950 nm range was detected by a GaAs photomultiplier (RCA 4832, rise time 10 ns), while near infra-red radiation (950-1700 nm) was monitored by a germanium semiconductor device (ADC model 403, response time 1 ms). The signals from the detectors were processed by a boxcar integrator (SRS 250) for the recording of emission and excitation spectra. Fluorescence decay curves were captured in real time by a transient recorder (LeCroy TR8837F) and signal averaged by a microcomputer (Zenith ZW 158). Photoselection measurements were made by exciting the samples with the linearly polarized light from the YAG laser. The detector was set to monitor vertically polarized radiation, and the polarization ratios were defined by the intensities observed for vertically and horizontally polarized excitation.

Results

(a) The $I_2 A^3\Pi(I_u) - X^1\Sigma_g^+$ System

Excitation of matrix isolated I_2 by wavelengths in the range of 530-725 nm resulted in strong emissions in the 1100-1700 nm region. Simple vibrational



For	
AI	<input checked="" type="checkbox"/>
ed	<input type="checkbox"/>
tion	<input type="checkbox"/>
tion/	
ility Codes	
ail and/or	
Special	

A-1

progressions were observed when the fluorescence emitted during the 100 μ s period following the laser pulse was detected. An example of the spectra obtained for I₂ in Ar (1:1000) is shown in Fig. 1. The qualitative features of this trace are representative of the spectra taken in all three matrix hosts. As is often observed with matrix isolated species, the emissions originated from the $v'=0$ levels of the excited states. The spectra obtained were essentially the same as those reported by Beeken et al.² in a similar study. They were readily assigned to the I₂ A \rightarrow X emission system. The positions of the band centers observed in the various matrix hosts are listed in Table 1. The intensity distributions and band centers were essentially independent of I₂ concentration for the range of dilutions investigated. For the spectra recorded in each matrix host, the ground state vibrational numberings were determined by trial fittings of the band centers to the equation

$$v = T_0 - \omega_e v'' + \omega_e x_e v''(v''+1)$$

In the absence of data for more than one isotopic species this procedure defines $\omega_e x_e$, but the vibrational numbering, T_0 , and ω_e are not uniquely determined. However, the ground state vibrational frequencies for I₂ isolated in Ar (213 cm⁻¹), Kr (210 cm⁻¹), and Xe (211 cm⁻¹) have been determined from Raman spectra by Howard and Andrews.³ When the fitting procedures were constrained to reproduce these vibrational frequencies the numberings were determined to within ± 2 units. Further refinements were obtained by comparing the fitted values of T_0 with the gas-phase results. Previous studies of halogens and interhalogens isolated in Ar matrices have shown that the T_0 values for the A³ $\Pi(1)$ and B³ $\Pi(0^+)$ states are decreased by 200-250 cm⁻¹ from their gas-phase values.^{4,11} When the fits to the Ar/I₂ (A-X) data were restricted to conform with this trend the numbering shown in Table 1 was uniquely determined. Table 2 gives the spectroscopic constants which resulted from this numbering.

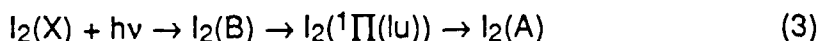
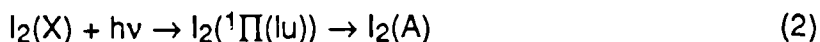
The gas-to-matrix shifts of T_0 induced by trapping halogens in Kr and Xe have not been characterized. On the basis of the behavior of a large number of other diatomic molecules, shifts which are approximately proportional to the polarizability of the host are expected.⁴ This trend has been observed for the $^2P_{1/2} \rightarrow ^2P_{3/2}$ transitions of matrix isolated iodine atoms (see below). Consequently, the fits to the I_2 (A-X) data were subjected to the additional constraint of $T_0(\text{Ar}) > T_0(\text{Kr}) > T_0(\text{Xe})$. The vibrational numberings derived from this scheme are given in Table 1. The corresponding constants and matrix shifts are given in Table 2.

Beeken et al.² have also analysed the I_2 A \rightarrow X bands observed in Ar and Xe matrices. Their vibrational assignments differed from those of Table 1 by one unit for Ar and two units for Xe. Beeken et al.² determined their numberings by minimizing the differences between the gas-phase and matrix T_0 values. This approximation is not consistent with the existing body of matrix data,⁴ or the behavior of matrix isolated iodine atoms.

The Ge detector was used to record fluorescence decay curves for the I_2 A \rightarrow X emissions. The response of this detector (4 μs rise time, 1 ms fall time) was relatively slow compared with the A state lifetime. As a consequence, the fluorescence decay was actually observed as a lengthening of the detector rise time.¹² Deconvolution of the time dependent signals yielded a lifetime of 50 ± 15 μs for all three matrix hosts. A slight tendency for the lifetime to shorten with increasing atomic mass of the host material was noted. These results are at variance with the measurements of Beeken et al.,² who observed lifetimes of 260 ± 30 μs for the same host materials. The source of this discrepancy is not clear at the present time. However, the longer lifetime is difficult to reconcile with the related observations for the A state of Br_2 . The gas-phase radiative lifetime of Br_2 (A) is 350 ± 50 μs .⁵ In Ar and Kr matrices the lifetime falls to 67 and 170 μs , respectively.⁶ A lifetime of 270 μs for I_2 (A) in an Ar matrix implies that, in the gas-

phase, the lifetime of $I_2(A)$ is comparable to, or greater than the lifetime of $Br_2(A)$. This is most unlikely. The decay rates of the A states reflect the magnitudes of spin-orbit coupling within the 2431 $^3\Pi$ states.⁵ This is greater in I_2 than in Br_2 . Based on spin-orbit coupling considerations, a matrix lifetime of about 100 μs would be expected for $I_2(A)$. The present matrix work is in reasonable agreement with this extrapolation.

Excitation spectra and polarization ratios were recorded in order to determine the mechanism by which absorption of light in the 530-580 nm region led to population of the A state. The possible excitation channels within this energy range are:



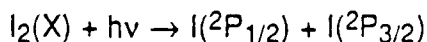
The I_2 B-X system has the strongest absorption in this spectral region, and in the gas-phase it is known that the B state is predissociated by the repulsive $^1\Pi(u)$ state. These observations suggest that channel (3) should provide the major route for population of the A state. However, in our previous study^{7,8} of the analogous process for Br_2 , we found that excitation of the B state did not lead to population of the A state. Channel (3) can be distinguished from channels (1) and/or (2) by measuring the polarization ratio.⁸ Under ideal conditions the former will yield a ratio of 1/2, while the latter will have a ratio of 4/3. In practice these ratios are modified by the depolarizing effects of the host material. A polarization ratio of 1.03 ± 0.01 was obtained by using 532 nm excitation and detection of the 1508 nm (0-20 band) emission. This was significantly greater than unity, indicating that processes (1) and/or (2) were dominant. The excitation spectrum, recorded by scanning the dye laser wavelength while monitoring the 0-20 band emission, was virtually flat over the range of 553-583 nm. This observation further supports the

conclusion that the B state excitation is not active in populating the A state. If it were, the B-X absorption, which rises steeply with decreasing wavelength at 560 nm, would be evident in the excitation spectrum. The "flat" response indicates that both the $^1\Pi(\text{lu})\text{-X}$ and A-X absorptions result in A-X emission. The conclusion that the B-X system is not active in this respect is at variance with the excitation mechanism proposed by Beeken et al.,² and the assumptions made by many investigators in the analyses of solution-phase I_2 recombination data.⁹

(b.) The $\text{I } ^2\text{P}_{1/2} - ^2\text{P}_{3/2}$ Transition

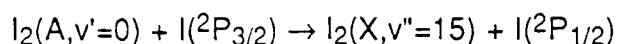
At I_2 : rare gas dilution ratios of 1:600 or less the atomic $\text{I } ^2\text{P}_{1/2} - ^2\text{P}_{3/2}$ transition was seen superimposed on the $\text{I}_2 \text{ A} \rightarrow \text{X}$ spectrum. The atomic line center, measured in Ar, Kr, and Xe matrices, is listed in Table 3. The line was red-shifted from its gas-phase value by an amount which was roughly proportional to the polarizability of the host.

The properties of I atoms isolated in I_2/Ar matrices were studied in the most detail. In this environment the $^2\text{P}_{1/2}$ state exhibited a lifetime of approximately 2 ms. A typical example of the emission spectrum from a 1:600, I_2 : Ar matrix is shown in Fig. 2. In order to enhance the atomic feature, this trace was recorded by monitoring the light emitted 2 ms after the laser pulse. Excitation wavelengths ranging from 532 to 725 nm produced the atomic emission, with an intensity that was linearly dependent on laser power. This implied that $^2\text{P}_{1/2}$ atoms were being produced by a single photon absorption, but by photons with insufficient energy for the process



An excitation spectrum was recorded by observing the atomic line and tuning the dye laser from 553-583 nm. The result was identical to the excitation spectrum recorded for the $\text{A} \rightarrow \text{X}$ system in low concentration matrices. Thus the atoms are

most probably excited by energy transfer from $I_2(A)$. From Fig. 2 it can be seen that the transfer will be near-resonant for the process



The presence of I atoms in the matrix is easily accounted for. The matrices were deposited under normal room lighting conditions, so the I_2 was subject to partial photodissociation before and during the deposition process. The probability of finding an I atom sufficiently close to an I_2 molecule for the energy transfer step will be quadratically dependent on concentration, which accounts for the observation that the atomic emission could only be seen with relatively concentrated samples.

Excitation of the $I(^2P_{1/2})$ state by transfer from $I_2(A)$ is a process which has not been reported previously, and may be of importance in the chemically pumped oxygen/iodine laser. From investigations of the kinetics of the laser it is known that appreciable concentrations of $I_2(A)$ are generated by energy transfer from $O_2(a)$.¹⁰ Previous models of the lasing kinetics have considered the role of $I_2(A)$ in the dissociation of I_2 , but its participation in the direct excitation of $I(^2P_{1/2})$ has never been examined. Clearly the present results indicate that studies of the gas-phase $I_2(A) + I$ system are needed for a more complete understanding of the lasing kinetics.

(c.) Energy Transfer from $I_2(A)$ to O_2

In a limited range of experiments, I_2 was co-deposited with O_2 in rare gas matrices. Excitation of these samples at wavelengths around 560 nm produced the $I_2(A-X)$, $I(^2P_{1/2} - ^2P_{3/2})$, and $O_2(a-X)$ emission systems. An example of the fluorescence spectrum, recorded by monitoring the light emitted 20 ms after the laser pulse, is shown in Fig. 3. Evidently the O_2 in the matrix perturbs the nearby I atoms to the extent that the atomic line is split into two components. The fluorescence decay lifetime of $O_2(a)$ was found to be very sensitive to the

conditions under which the matrix was deposited. Typically, lifetimes of 1 to 5 seconds were observed. The excitation spectrum, obtained by monitoring the $O_2(a-X)$ transition as the laser wavelength was varied, was identical to the $I_2(A)$ excitation spectrum. Thus it appears that $O_2(a)$ is populated by energy transfer.

The lifetime of $I(^2P_{1/2})$ in rare gas matrices was found to be ≤ 2 ms. Detection of the atomic emission after a decay time of 20 ms indicates that the atoms are being excited by energy transfer from $O_2(a)$. This process is directly analogous to the gas-phase $O_2(a) \rightarrow I^*$ transfer.

(III.) Radiative Lifetime Measurements for the $B^3\Pi(O^+)$ State of ClF

In an earlier report, the first attempts to measure the gas-phase radiative lifetime of ClF(B) by LIF techniques were described. This measurement is technically difficult because the B-X transition is weak, and the B state is expected to be long-lived ($\tau > 100 \mu s$). The long life time necessitates the use of pressures below 1 mTorr for effectively collision-free observations. With such low pressures, and a small absorption strength, the LIF signals are extremely weak. Contamination of the ClF sample by tiny amounts of a strongly fluorescent species can seriously bias the results. In addition, at pressures below 1 mTorr the ClF(B) molecules can diffuse large distances before they radiate. Molecules may travel beyond the volume viewed by the detector, or they may be deactivated on the walls of the chamber, thereby causing an artificial shortening of the lifetime.

Our first determination of the B state lifetime produced a surprisingly small value ($30 \pm 10 \mu s$), and it was suspected that the results were subject to large systematic errors. The major problem in these experiments was the presence of a strongly fluorescent contaminant in all of the ClF samples. Fluorescence from this species could not be avoided as its LIF spectrum was continuous in the region where ClF absorbs. Attempts to "trap out" the impurity, by passing the ClF through copper coils immersed in a dry ice shush bath, were unsuccessful. The fluorescence decay lifetime of the impurity was measured by exciting at wavelengths which were not resonant with ClF transitions. An approximate lifetime of $1 \mu s$ was obtained. Using this information it was judged that the ClF(B) fluorescence would be effectively free from interference after $10 \mu s$. Unfortunately, further investigation has shown that the impurity fluorescence does not decay exponentially, and that it possesses a fairly long-lived tail ($\tau \approx 30 \mu s$). The contribution of this signal to the ClF decay, at times greater than $10 \mu s$ after the laser pulse, lead to a serious underestimation of the lifetime.

The initial studies were conducted with a laser linewidth of 0.3 cm^{-1} , which was much broader than the Doppler linewidth for ClF at room temperature (0.03 cm^{-1}). As the absorption by the impurity was continuous, the broad laser linewidth was exciting this species more efficiently than the ClF. The situation was improved by using an intra-cavity etalon to reduce the laser linewidth to 0.05 cm^{-1} . Excitation spectra for ClF, recorded with the line-narrowed laser, are shown in Figures 4 and 5. The sloping baselines in these spectra were caused by the impurity fluorescence, but the ratio of ClF to impurity signal was greatly improved by the reduced linewidth. Subtraction techniques were used to compensate for the remaining background fluorescence. With a stable pressure of ClF in the vacuum chamber, the laser was tuned into resonance with an isolated rotational feature. A fluorescence decay curve was recorded by signal averaging for 10,000 to 30,000 laser pulses. The laser was then detuned from the resonance, and the background signal was averaged for an equivalent number of pulses. The result was subtracted from the on-resonance signal, leaving the component which belonged to ClF(B). Decay curves were recorded by this method for total ClF pressures ranging from 0.9-40 mTorr. The B state levels examined were $v'=5, J'=16$; $v'=7, J'=10$; and $v'=7, J'=14$.

Care was needed in the analysis of the low pressure ($<5\text{ mTorr}$) data, as diffusion could affect the latter part of the decay. The positioning of the photomultiplier was such that it could observe a sphere of 10.6 cm radius inside the chamber. Excited molecules which diffused beyond this radius could not be detected. At 1 mTorr the average diffusion rate carries the molecules 10 cm in 500 μs , so the data were analyzed for the first 350 μs after the laser pulse. Even with the observation time restricted to this upper limit, complex (non-exponential) decays were obtained in many of the measurements. Vibrational relaxation within the B state manifold was responsible for an instrumental distortion of the decay

curve. The photomultiplier, which was screened from scattered laser light by a long-pass filter, had a strongly wavelength dependent sensitivity. Time dependent changes in the fluorescence spectrum, caused by vibrational relaxation, modified the efficiency with which the excited molecules were detected. This process was convoluted with the exponential radiative relaxation, producing a complex decay curve.² The problem was minimized by choosing a photomultiplier/long-pass filter combination that had an almost constant detection efficiency for levels in the range of $4 \leq v' \leq 7$. An EMI 9558 photomultiplier, screened by a Hoya 0-56 filter, gave good single exponential decays on a 0-350 μ s timebase.

A Stern-Volmer plot, constructed from the measurements for all of the levels examined, is shown in Figure 6. Linear least squares fitting to this data gave a collision-free lifetime of 300 ± 50 μ s and a self deactivation rate constant of 2.3×10^{-11} cm^3 molecule⁻¹ s⁻¹. The lifetime is comparable to that reported for the Cl₂ B state (305 ± 15 μ s)² and it defines an electronic transition dipole of $|R_e|^2 = (1.0 \pm 0.3) \times 10^{-2}$ D².

Preliminary calculations, based on the above value for $|R_e|^2$, indicate that lasing of the ClF B-X transition can be achieved by optical pumping. The most favorable approach involves excitation of the 6-0 band and lasing of the 6-4 transition at 576 nm. The latter has a stimulated emission cross section of 4.7×10^{-17} cm², providing a gain of 1.02 cm⁻¹ for an excited state density of 4×10^{14} molecules cm⁻³. Optical pumping of a natural isotopic mixture of ClF at a total pressure of 2 Torr will produce this excited state density. The pump laser needed for saturation of the 6-0 transition must have a pulse energy of 10 mJ (in a 10 ns pulse), linewidth of 0.06 cm⁻¹, and a beam diameter of 0.1 cm. These requirements are easily met or exceeded using commercially available dye laser systems.

(IV.) Resolved Fluorescence Studies of the Collision Dynamics of Br₂ (B)

The fluorescence decay dynamics of the Br₂ B state have been studied in detail by time-resolved fluorescence techniques. This work is briefly summarized in reference 13. The main conclusions drawn from these studies were:

- (i) The B state is subject to a rotationally dependent predissociation. Within a given vibrational manifold the collision-free decay rate is given by

$$\Gamma_0 = \Gamma_r + C_V^2 J(J+1),$$

where Γ_r is the radiative decay rate and C_V^2 is the gyroscopic predissociation rate constant.

- (ii) Electronic self quenching of the levels with $v' \geq 4$, $J' \geq 20$ occurs with a rate constant of $1.4 \times 10^7 \text{ s}^{-1} \text{ Torr}^{-1}$. The dominant quenching mechanism is thought to be collision-induced predissociation.
- (iii) The self quenching kinetics of the low J' (≤ 15) levels of $v'=11$ and 14 are complex. The decay rates show non-linear dependencies on bromine pressure in the 0-1 Torr range.

In the past, the convoluted decay kinetics of the low J' levels have been interpreted in terms of a deactivation mechanism which involves rapid energy transfer to strongly predissociated levels. Computational modelling of this process indicated that both rotational and vibrational energy transfer were highly probable events in Br₂(B) + Br₂(X) collisions.¹³ The rate for loss of population from a single ro-vibronic level by electronic quenching and energy transfer was estimated to be $4.5 \times 10^7 \text{ s}^{-1} \text{ Torr}^{-1}$. This is significantly greater than gas kinetic, and difficult to reconcile with the performance of the optically pumped Br₂ (B-X) laser.¹⁴ Based on a model of the Br₂ laser kinetics, Perram and Davis¹⁴ have suggested that the upper limit for the total removal rate constant is $8.1 \times 10^6 \text{ s}^{-1} \text{ Torr}^{-1}$.

In order to investigate these discrepancies further, wavelength-resolved fluorescence techniques have been used to study the Br₂ B state. Continuous

wave excitation of isolated ro-vibrational states was used to observe energy transfer processes, and to measure the deactivation rate constants by the classical Stern-Volmer approach. The principle findings of this work were:

- (i) The collision dynamics of Br_2 (B), $v' \geq 4$ are dominated by electronic deactivation. The quenching rate constants measured by both steady-state and time-resolved fluorescence techniques are in good agreement for the levels with $J > 15$.
- (ii) Rotational energy transfer occurs in the $v' = 11$ and 14 manifolds with a rate constant of approximately $2 \times 10^6 \text{ s}^{-1} \text{ Torr}^{-1}$.
- (iii) Vibrational energy transfer is relatively inefficient ($k_v < 1 \times 10^6 \text{ s}^{-1} \text{ Torr}^{-1}$) for $v' = 11$ and 14.

EXPERIMENTAL

The experimental component of this work was carried out at AFWL, in collaboration with Drs. E. Dorko, G. Perram, and Mr. L. Hanko. The apparatus used for this work is shown in Figure 7. A similar system has been described in detail by Perram.¹⁵ A natural isotopic mixture of Br_2 was transferred into the previously evacuated fluorescence cell. The pressure in the cell was measured using capacitance monometers (Baratron 0-1 and 0-10 Torr sensors), and varied between 0.005 and 10 Torr. The B-X transition was excited by the light from a CW dye laser (Coherent 699, linewidth 500 kHz). Absolute wavenumber calibration of the laser was provided by deflecting a small fraction of the beam into a wavemeter. The laser was brought into resonance with a specific ro-vibronic transitions by first coarse tuning to the known wavenumber position of the line, and then fine tuning to maximize the fluorescence intensity. For this purpose a photomultiplier, shielded from scattered laser light by a long-pass filter, was used to monitor the undispersed emission. A 0.3 m monochromator was used to spectrally resolve the fluorescence. Light from the excitation zone was imaged onto the monochromator entrance slit.

In most experiments a slit width of 20 μm was used, resulting in a resolution of 0.6A. The dispersed fluorescence was detected by a cooled photomultiplier which was operated in a photon counting mode.

Self deactivation was studied by monitoring the intensity of emission from the optically excited state as a function of Br_2 pressure. For example, to characterize the deactivation of $v'=11$, $J'=35$ the laser was tuned to the 11-1, R(34) line, and the monochromator was set to transmit the 11-4, P(36) emission. Energy transfer was investigated by observing the pressure dependence of the resolved fluorescence spectrum.

RESULTS

(a) Self Deactivation

The fluorescence intensity vs Br_2 pressure data can be analyzed using a simple kinetic model. The rate of change in the population of the optically excited state is given by

$$\frac{d[\text{Br}_2(v',J')]}{dt} = I_L B g [\text{Br}_2]_0 - (I_L B + \Gamma_0 + k_T [\text{Br}_2]_0) [\text{Br}_2(v',J')]$$

where $[\text{Br}_2]_0$ is the concentration of ground state molecules, g is the fraction of molecules which can undergo excitation, B is the Einstein coefficient of the transition excited, I_L is the laser intensity, Γ_0 is the collision-free decay rate, and k_T is the rate constant for removal of population from the state v',J' . The measurements were conducted under steady state conditions ($d[\text{Br}_2(v',J')]/dt=0$), so the above expression can be rearranged to give

$$\frac{I_L B g [\text{Br}_2]_0}{[\text{Br}_2(v',J')]} = I_L B + \Gamma_0 + k_T [\text{Br}_2]_0$$

The dispersed fluorescence intensity from $\text{Br}_2(v',J')$, F , is directly proportional to $\Gamma_f [\text{Br}_2(v',J')]$. Replacing concentration by pressure, and assuming that a very small fraction of the molecules undergo excitation, we have

$$\frac{I_L P}{F} = A(I_L B + \Gamma_0 + k_T P) \quad \dots \dots \text{Eq (1)}$$

where P is the total Br_2 pressure and A is a constant. Consequently, a plot of $I_L P/F$ vs P (equivalent to the classical Stern-Volmer plot) should be linear, and the ratio of the slope to the intercept defines $k_T/(I_L B + \Gamma_0)$. If $I_L B + \Gamma_0$ is known, k_T can be determined without evaluating A . Matters are simplified further when it is possible to work under conditions where $I_L B \ll \Gamma_0$.

Figures 8 and 9 show typical plots of the fluorescence intensity data for $\text{Br}_2(\text{B})$, $v'=11$. The results are well represented by Eq (1). The total removal rate constants for $\text{Br}_2(\text{B})$, $v'=11$, determined by fitting to Eq (1), are given in Table 4. In each case the measurements were made at a number of different laser intensities, in order to assess the magnitude of the term $I_L B$. No contributions from this term were detected for laser powers below 110 mW. This fact is illustrated by the results for $v'=11$, $J'=4$, which are given in Table 5. Particular attention was paid to the emission from this level because it has a very small collision-free decay rate, and is therefore most likely to be influenced by stimulated emission. In addition, the value of k_T determined for this level by steady-state methods appears to be anomalously low.

Self deactivation of $\text{Br}_2(\text{B})$, $v'=14$ was examined by exciting the P(5) and R(36) lines of the 14-2 band. The results for P(5), summarized in Table 6, showed a distinct dependence on the laser intensity. This dependence is illustrated in Figure 10. Further evidence that the results for P(5) were influenced by stimulated emission was obtained by observing the fluorescence intensity as a function of laser intensity at a fixed Br_2 pressure. As Figure 11 shows, saturation of the P(5), 14-2 transition caused a non-linear dependence of F on I_L at powers above 10mW. The 14-2 band is more easily saturated than the 11-1 band because it has a much larger Franck-Condon factor ($q_{11-1} = 0.0017$, $q_{14-2} = 0.017$).

(b) Rotational Energy Transfer

Figure 12 shows an example of the resolved fluorescence data. This spectrum is dominated by the two lines which correspond to emission from the initially excited (parent) state. Weaker features, which occur on either side of the parent lines (c.f. Figure 13), are emitted by collisionally populated levels. Treating the energy transfer as a single collision event, and assuming a constant collision-free decay rate for the range of rotational states observed, it is easy to show that the ratio of population in a collisionally excited level to that of the parent level is given by

$$\frac{[Br_2(v', J' + \Delta J)]}{[Br_2(v', J')]} = \frac{k(J' \rightarrow J' + \Delta J)[Br_2]_0}{(\Gamma_0 + k_T[Br_2]_0)}$$

where $k(J' \rightarrow J' + \Delta J)$ is the energy transfer rate constant. In the high pressure limit, where $k_T[Br_2]_0 \gg \Gamma_0$, the ratio reduces to $k(J' \rightarrow J' + \Delta J)/k_T$.

Rotationally resolved fluorescence spectra were recorded by exciting the P(5), R(5), R(10), P(18), R(22), P(30), R(34), and R(43) lines of the 11-1 band. For each line the spectrum was observed at pressures ranging from 0.02 to 10 Torr. A preliminary analysis of these data provides an estimate for the sum of the rotational energy transfer rate constants, $k_{RT} = \sum_{\Delta J} k(J' \rightarrow J' + \Delta J)$, of $2 \times 10^6 s^{-1} Torr^{-1}$. Weak emission from collisionally populated vibrational levels was also detected. The intensity data for these bands have not been analyzed quantitatively, but qualitatively it is clear that vibrational energy transfer is slow compared to quenching and rotational energy transfer. The band contours indicate that the angular momentum is approximately conserved in vibrationally inelastic collisions. Detailed analyses of the resolved fluorescence spectra are currently in progress.

Discussion

The present study provides an average deactivation rate constant of $1.6 \times 10^7 \text{ s}^{-1} \text{ Torr}^{-1}$ ($4.9 \times 10^{-10} \text{ cm}^3 \text{ molecule}^{-1} \text{ s}^{-1}$) for the $J' > 15$ levels of $v' = 11$ and 14. This result is in excellent agreement with the value obtained from the time-resolved measurements. However, both steady-state and time-resolved measurements reveal anomalous behavior of the $J' < 15$ levels. Moreover, the results from these two techniques appear to be incompatible. Tables 4, 5, and 6 show that the steady-state measurements yield deactivation rate constants which decrease with decreasing rotational energy. Conversely, the time-resolved measurements, made at pressures below 100 mTorr, define deactivation rate constants which increase with decreasing energy. The low magnitudes of the energy transfer rate constants determined in the present study lead to the conclusion that these trends cannot be interpreted using energy transfer models. Experiments which combine time- and wavelength-resolved fluorescence techniques are needed to shed further light on these apparent anomalies.

References

1. J. P. Nicolai and M. C. Heaven, J. Chem. Phys. 87, 3304 (1987)
2. P. B. Beeken, E. A. Hanson, and G. W. Flynn, J. Chem. Phys. 78, 5892 (1983)
3. W. F. Howard and L. Andrews, J. Raman. Spectrsc. 2, 447 (1974)
4. M. E. Jacox, J. Mol. Struct. 157, 43 (1987)
5. M. C. Heaven, Chem. Soc. Rev. 15, 405 (1986)
6. M. Mandich, P. Beeken, and G. Flynn, J. Chem. Phys. 77, 702 (1982)
7. J. P. Nicolai, L. J. van de Burgt and M. C. Heaven, Chem. Phys. Lett. 115, 496 (1985)
8. J. P. Nicolai and M. C. Heaven, J. Chem. Phys. 83, 6538 (1985)
9. see N. Alan, Abul-Haj and D. F. Kelley, J. Chem. Phys. 84, 1335 (1986), and references therein
10. see G. E. Hall, W. J. Marinelli, and P. L. Houston, J. Phys. Chem. 87, 2153 (1983), and references therein
11. J. Langen, K-P. Lodemann, and U. Schurath, Chem. Phys. 112, 393 (1987)
12. J. N. Demas, Excited State Lifetime Measurements (Academic Press, NY 1983)
13. L. J. van de Burgt and M. C. Heaven, Chem. Phys. 103, 407 (1986)
14. G. P. Perram and S. J. Davis, J. Chem. Phys. 84, 2526 (1986)
15. G. P. Perram, Ph.D. Thesis, AFIT, 1986

Table 1

Vibronic Band Positions (cm^{-1}) of the A-X System of I_2 in Solid Rare Gas Matrices

$v'=0 \rightarrow v''$	$\nu(\text{Ar})$	$\nu(\text{Kr})$	$\nu(\text{Xe})$
10	8547	8503	
11	8345	8306	8183
12	8155	8112	7994
13	7960	7915	7806
14	7766	7723	7616
15	7576	7534	7429
16	7383	7344	7241
17	7190	7154	7057
18	7005	6970	6873
19	6816	6784	6690
20	6631	6600	6510
21	6449	6417	6332
22	6264	6233	6156
23	6082	6056	5979
24	5902	5876	5806
25		5698	

Table 2

Spectroscopic Constants (cm^{-1}) for the A-X System of I_2 in Solid Rare Gas Matrices

Matrix Host	ω_e''	$\omega_e x_e''$	$T_e(A)$	Δ^a
Ar	213	0.67	10661	246
Kr	212	0.69	10602	305
Xe	209	0.72	10448	459
gas-phase	214.5	0.61	10906.8	

a. Δ is the difference between the gas-phase and matrix values of $T_e(A)$.

Table 3

Line Centers for the I $^2P_{1/2} - ^2P_{3/2}$ Transition in Ar, Kr, and Xe Matrices

Matrix Host	$\nu_0(\text{cm}^{-1})$	Matirx Shift (cm^{-1})
Ar	7564	41
Kr	7541	64
Xe	7502	103
gas-phase	7605	

Table 4

Self Deactivation of $^{79}\text{Br } ^{81}\text{Br}$, $\text{B}^3\Pi (\text{O}_\text{u}^+)$, $v'=11$

Line ^a	J'	$\Gamma_\text{O}^\text{b}/10^6 \text{ s}^{-1}$	$k_\text{T}/\Gamma_\text{O}(\text{Torr}^{-1})$	$k_\text{T}/10^7 \text{ s}^{-1} \text{ Torr}^{-1}$
R(4)	5	0.42	17	0.71
R(5)	6	0.47	22	1.0
R(10)	11	1.0	13	1.3
R(21)	22	4.8	3.4	1.6
R(21)	22	4.8	3.2	1.5
P(30)	29	7.0	2.0	1.4
R(34)	35	10	1.6	1.6
R(34)	35	10	1.6	1.6
R(34) ^c	35	10	1.7	1.7

^aTransitions of the 11-1 band.^bDecay rates from M. A. A. Clyne and M. C. Heaven, JCS Faraday II, 74, 1992 (1978).^cDetection of unresolved fluorescence.

Table 5

Self Deactivation of $\text{Br}_2 \text{B}^3\Pi (\text{O}_u^+)$, $v'=11$, $J'=4$ $^{79}\text{Br } ^{81}\text{Br}; \Gamma_0 = 3.0 \times 10^5 \text{ s}^{-1}$

Slit width/ μm	I_L/mW	$k_T/\Gamma_0(\text{Torr}^{-1})$	$k_T/10^7 \text{ s}^{-1} \text{ Torr}^{-1}$
20	6	18	0.54
20	70	18	0.54
20	90	21	0.63
20	100	20	0.60
20	110	24	0.72
20 ^a	26	17	0.51
200	55	23	0.69

 $^{81}\text{Br } ^{81}\text{Br}; \Gamma_0 = 3.0 \times 10^5 \text{ s}^{-1}$

20	94	22	0.72
----	----	----	------

^aDetection of unresolved fluorescence.

Table 6

Self Deactivation of $^{79}\text{Br } ^{81}\text{Br}$, $\text{B}^3\Pi (\text{O}_\text{U}^+)$, $v'=14$

Line ^a	J'	I _L /mW	$\Gamma_\text{O}^b/10^6 \text{ s}^{-1}$	$k_\text{T}/\Gamma_\text{O}(\text{Torr}^{-1})$	$k_\text{T}/10^7 \text{ s}^{-1} \text{ Torr}^{-1}$
P(5)	4	87	0.27	5.3	0.14
P(5)	4	60	0.27	5.5	0.15
P(5)	4	18	0.27	9.2	0.25
P(5)	4	3	0.27	12	0.33
R(36)	37	8	9.4	1.5	1.4
R(36)	37	1	9.4	1.7	1.6

^aTransitions of the 14-2 band^bDecay rates from M. A. A. Clyne and M. C. Heaven, JCS Faraday II, 74, 1992 (1978).

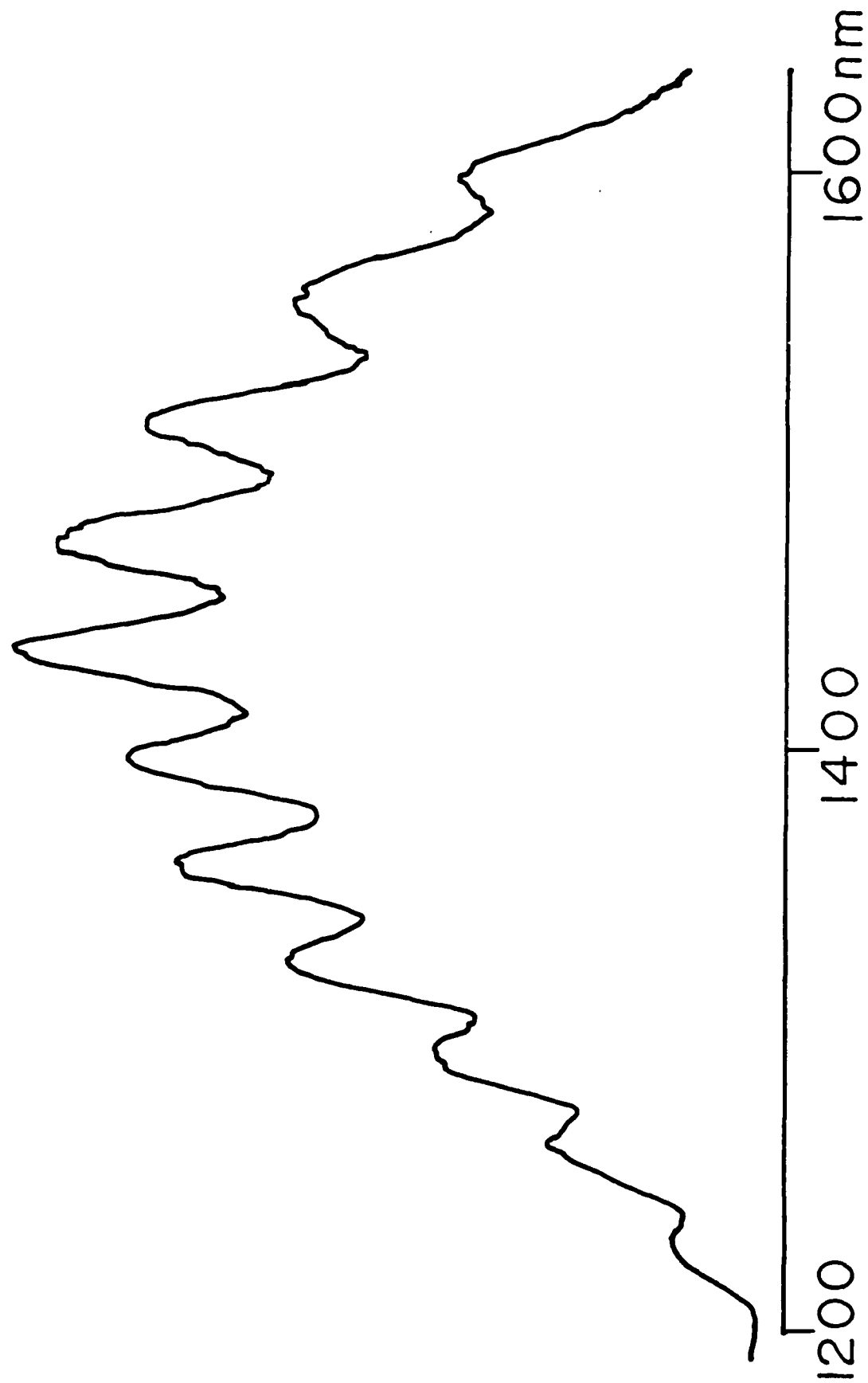


Figure 1.

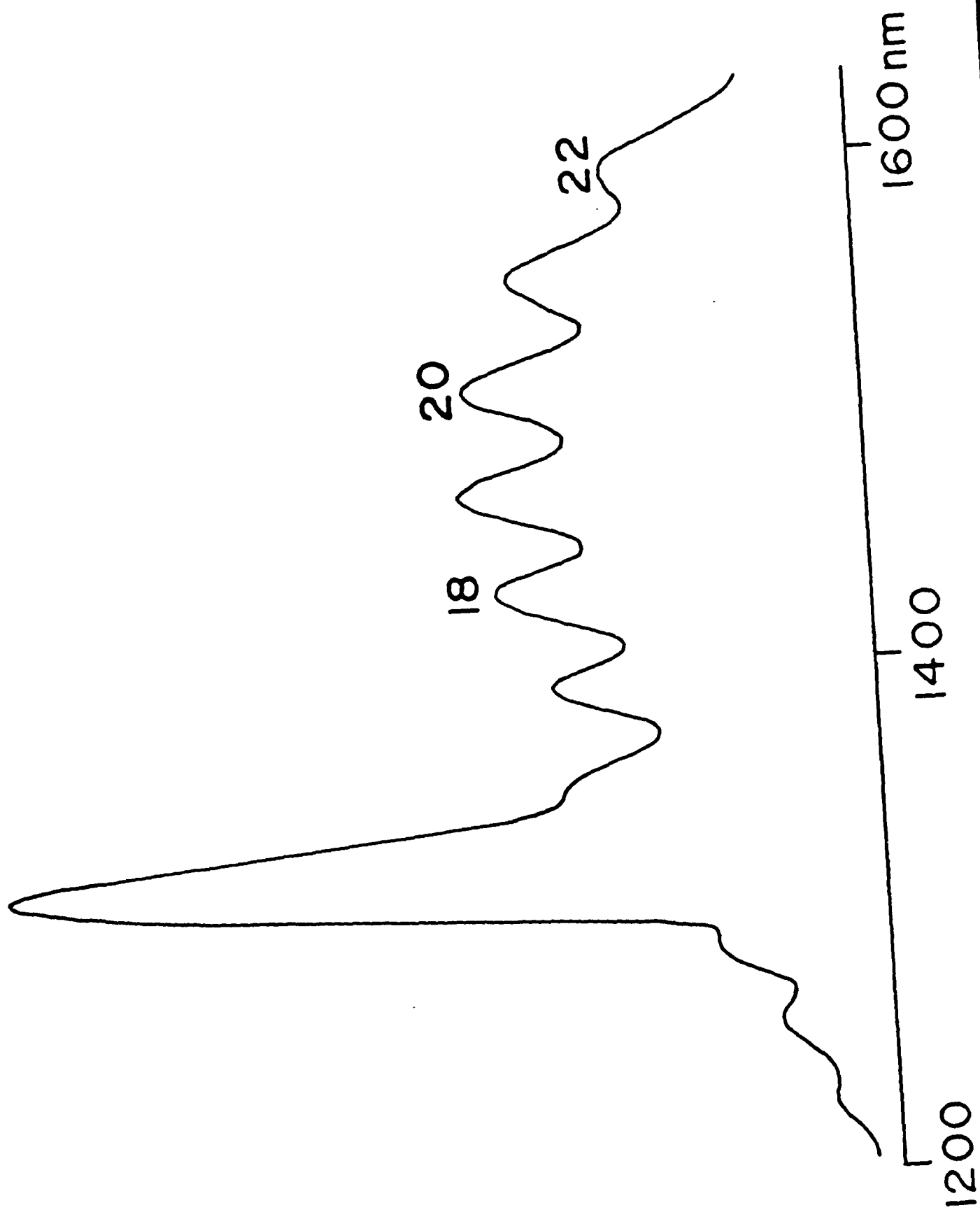


Figure 2.

$\text{O}_2 \text{ a}^1\Delta - \text{X}^3\Sigma$

$\text{I } ^2\text{P}_{1/2} - ^2\text{P}_{3/2}$

1400

1300

(nm)

1200

Figure 3.

CIF 5 - 0

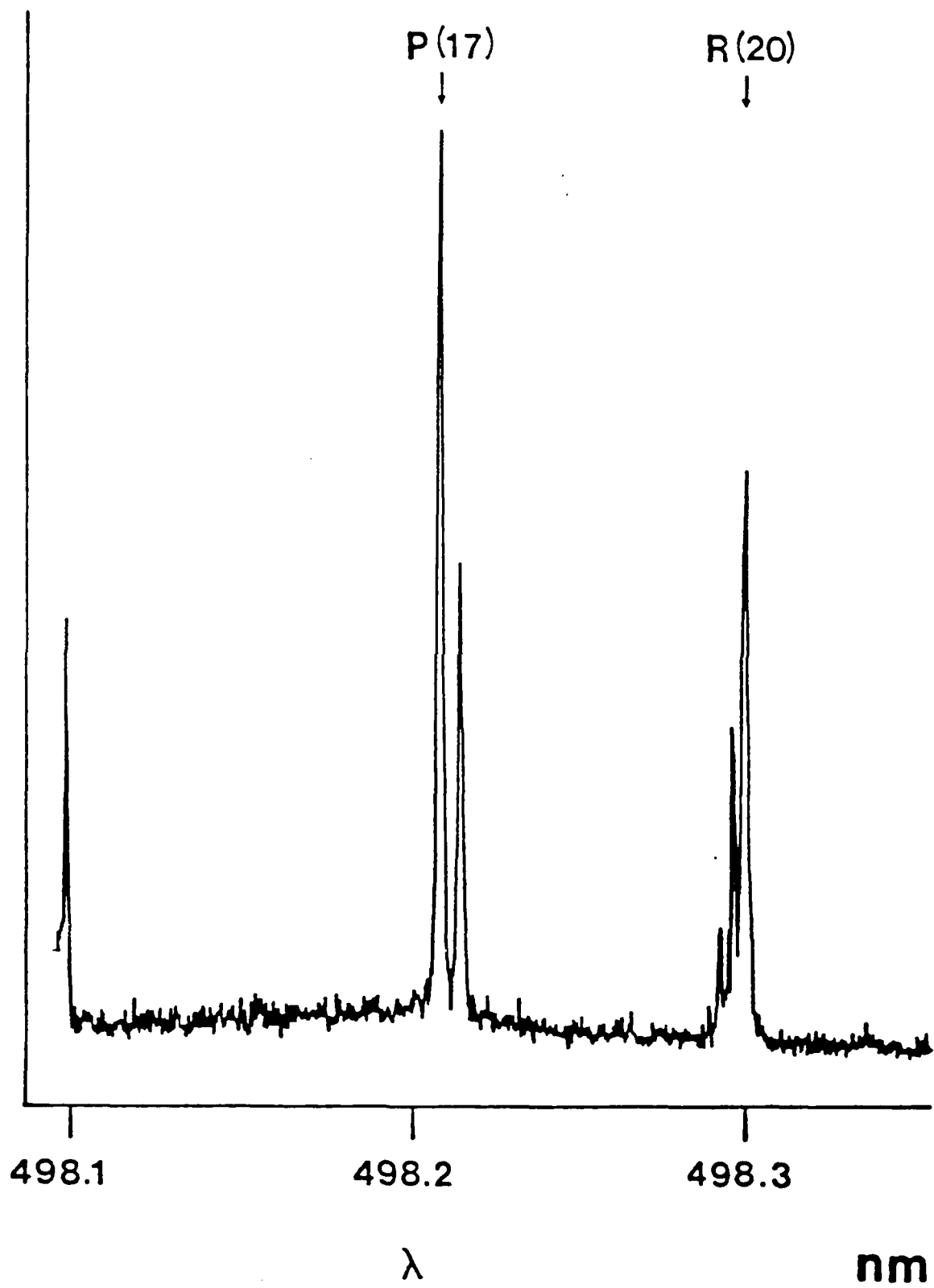


Figure 4.

CIF 7-0

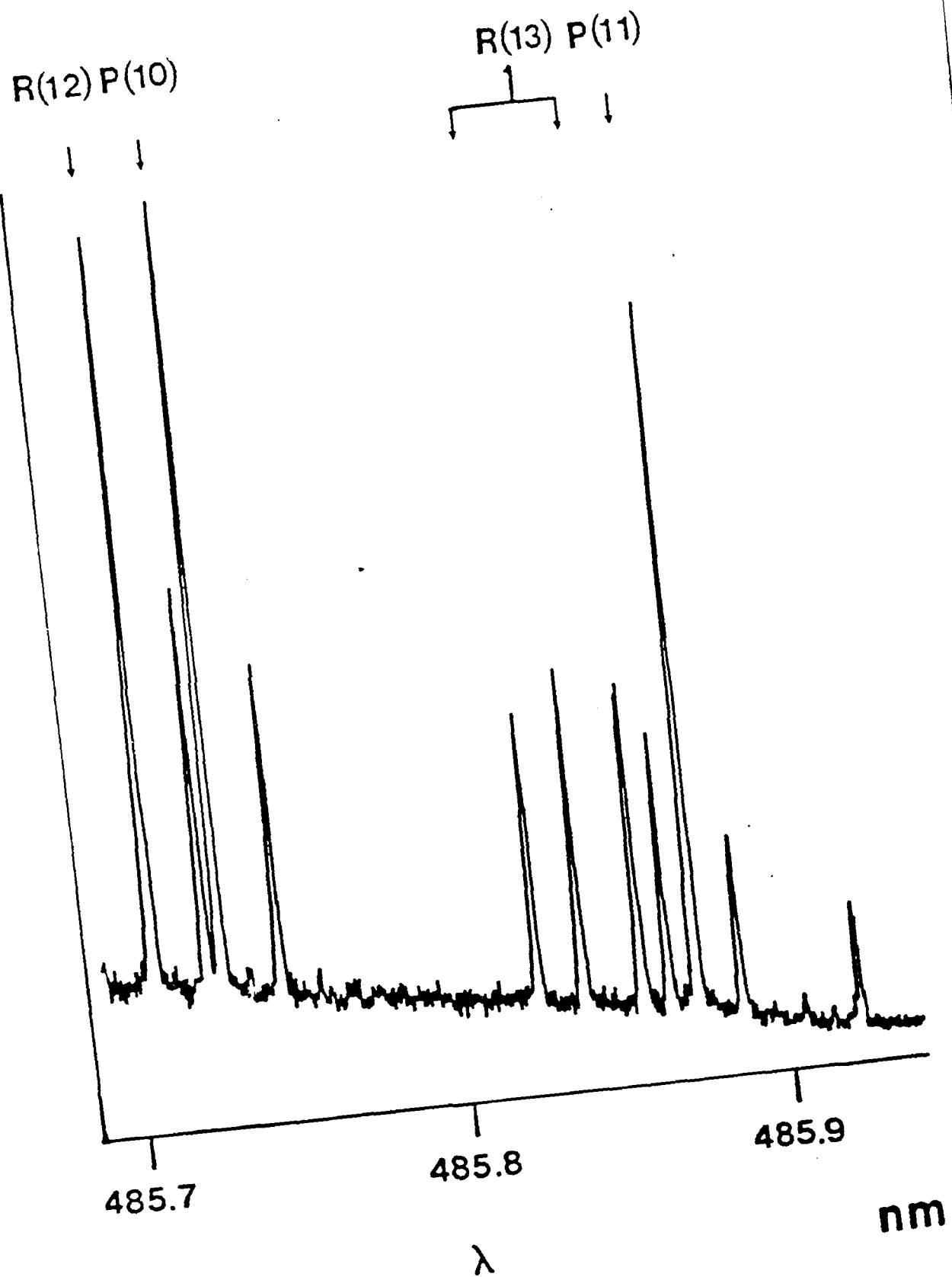


Figure 5.

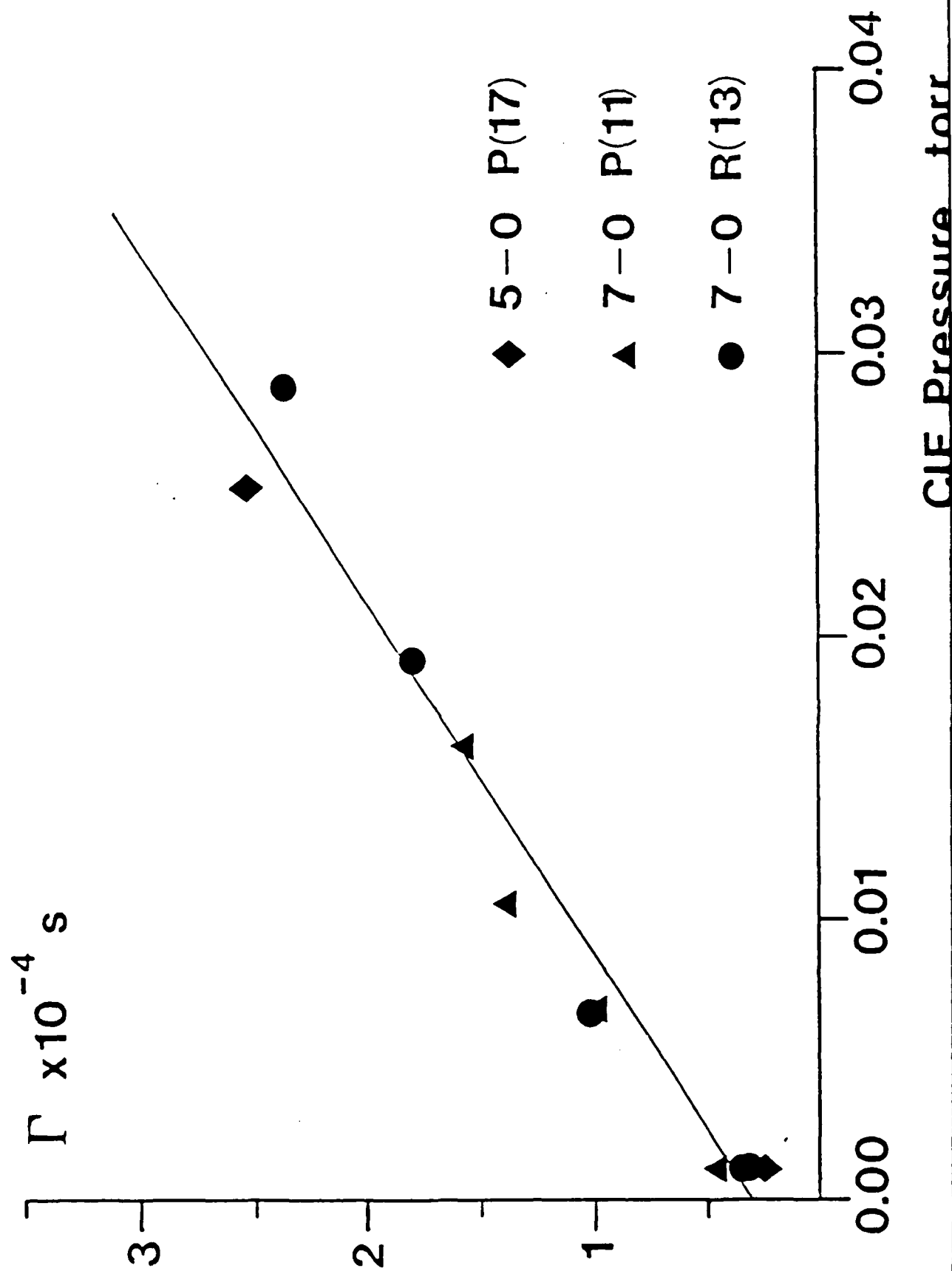


Figure 6.

CW SPECTRALLY RESOLVED FLUORESCENCE

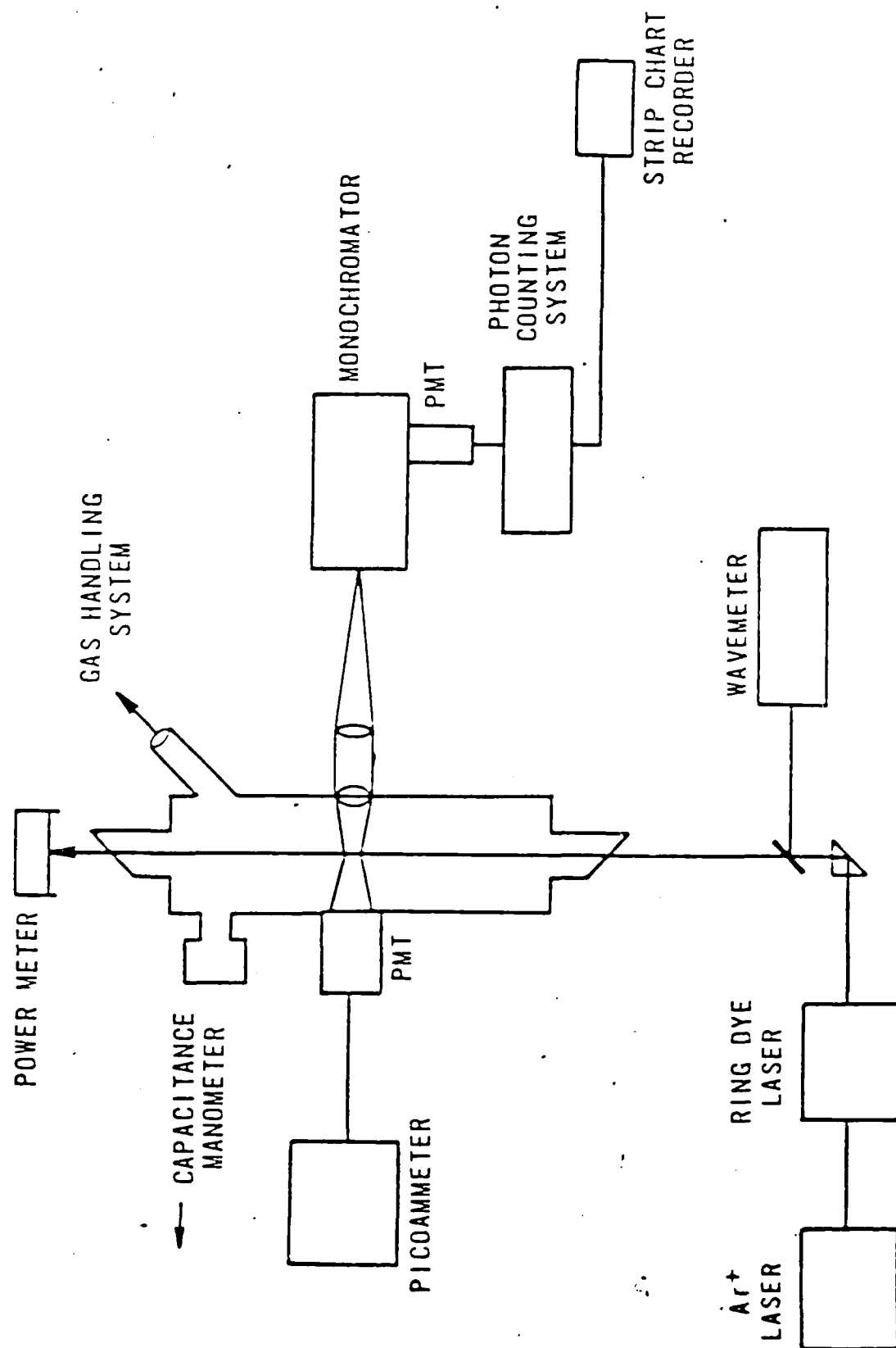


Figure 7.

Stern-Volmer Plot. $v' = 11$, $J' = 4$

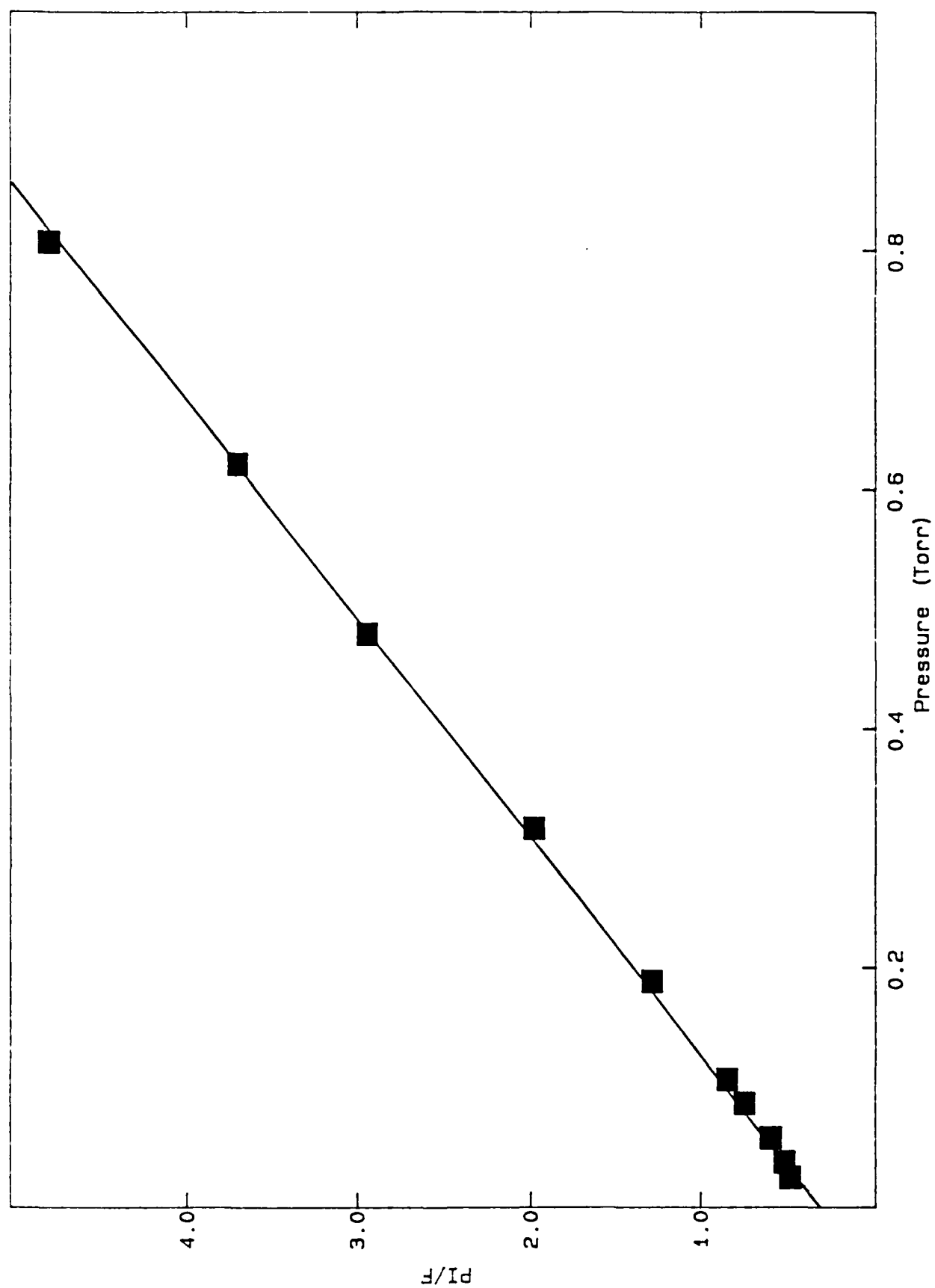


Figure 3.

Stern-Volmer Plot. $v'=11$, $J'=35$

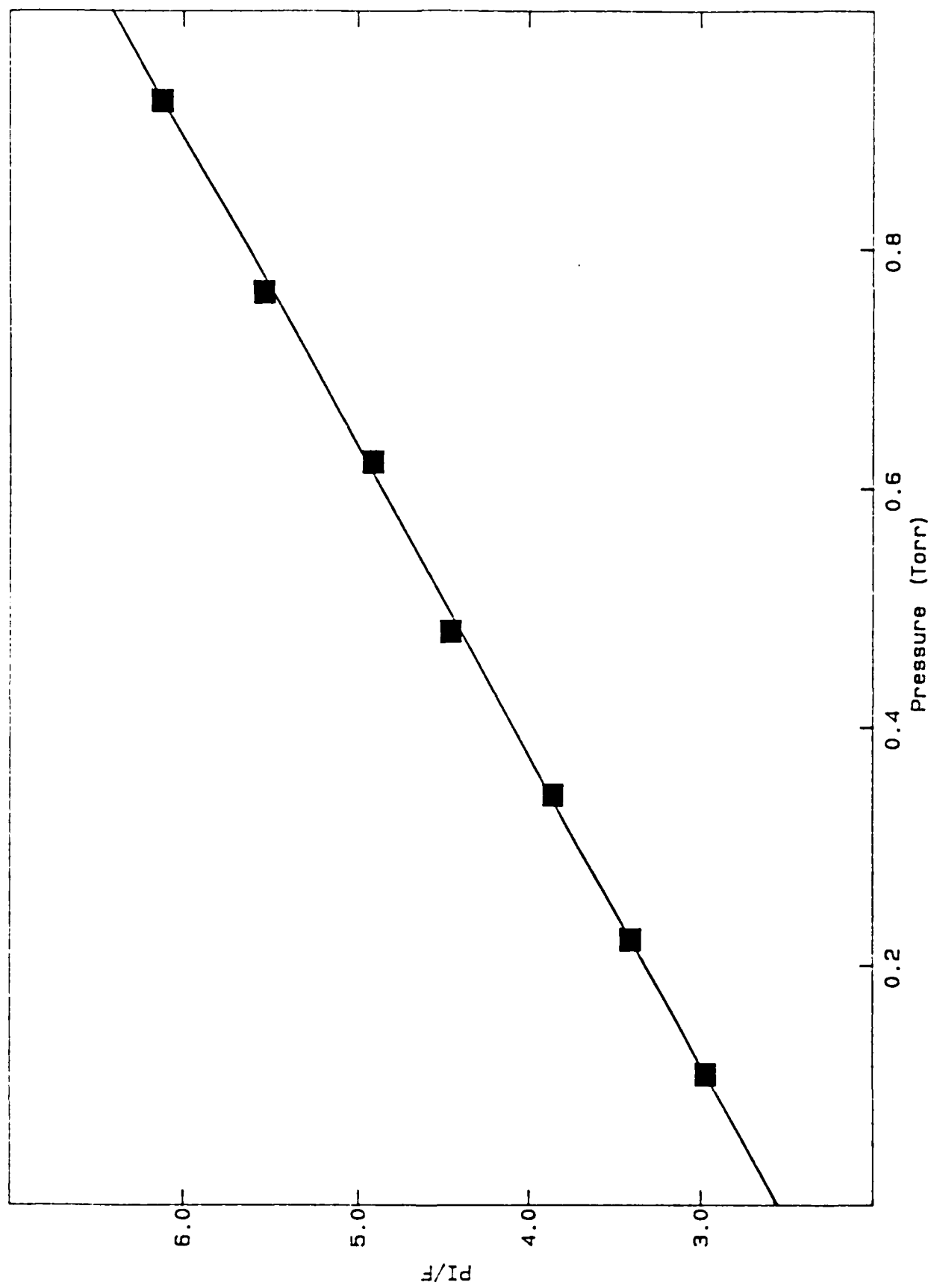


Figure 9.

Stern-Volmer Plots. $v'=14$, $J'=4$

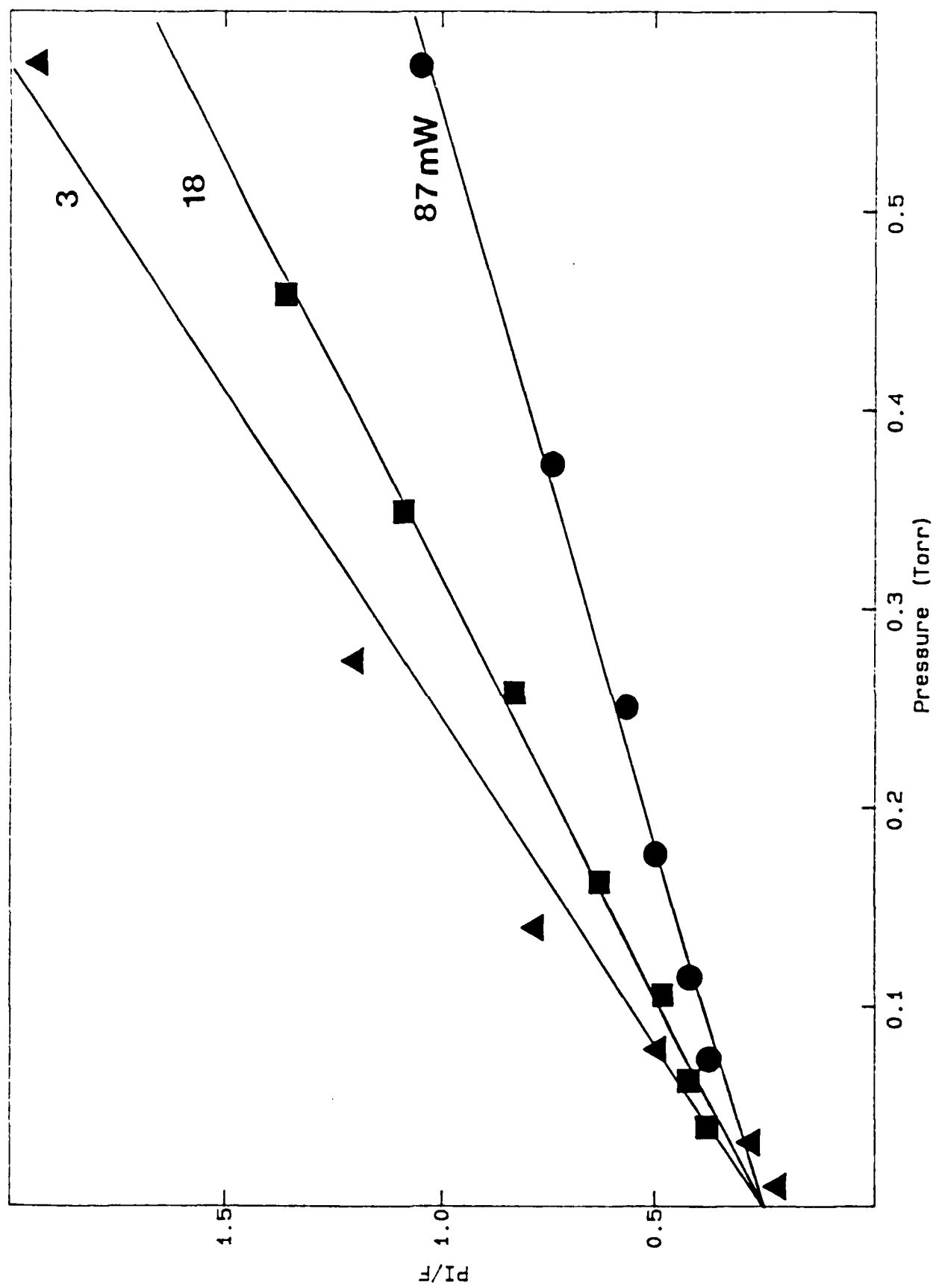


Figure 10.

$V' = 14, J' = 4$

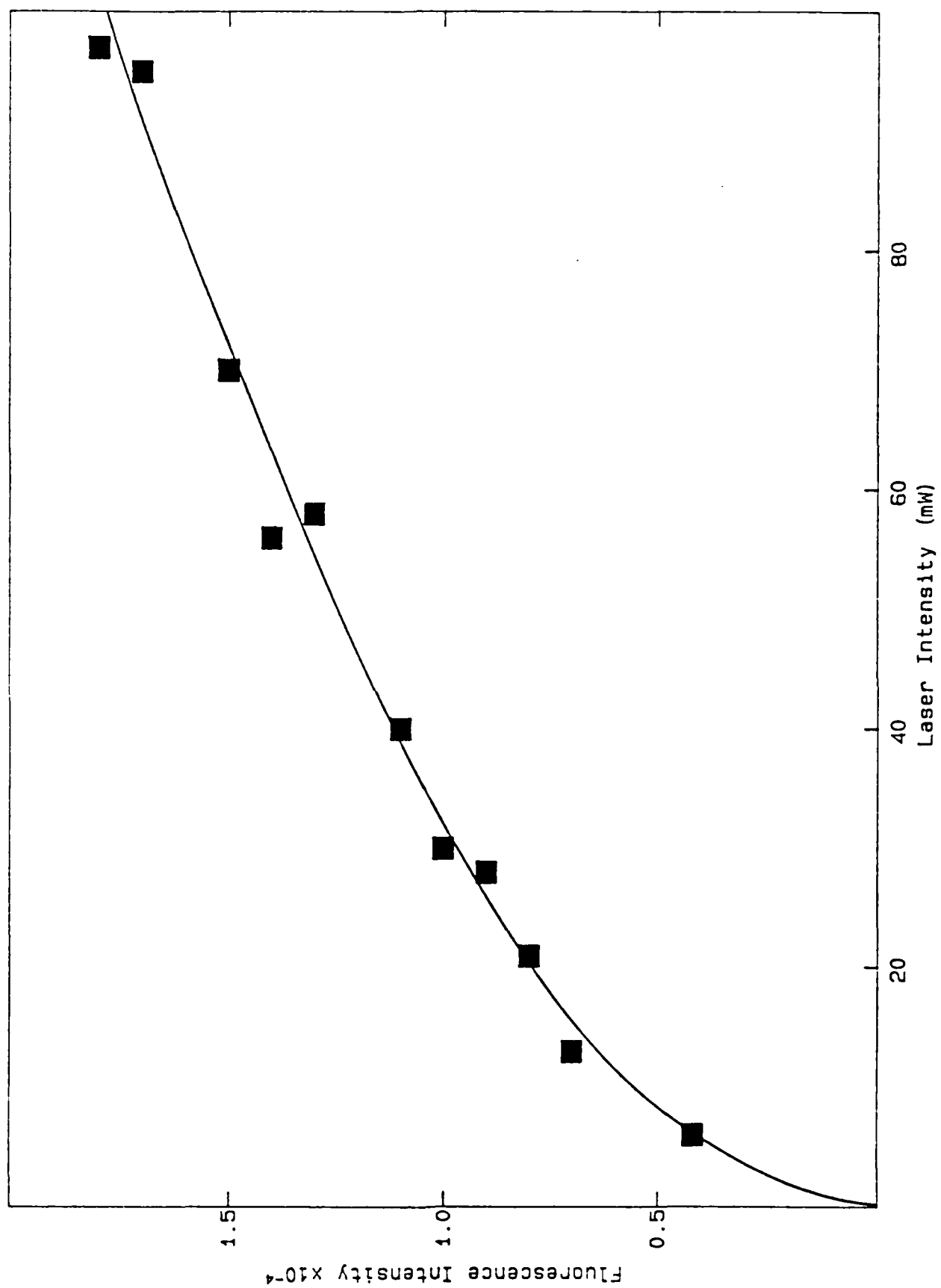


Figure 11.

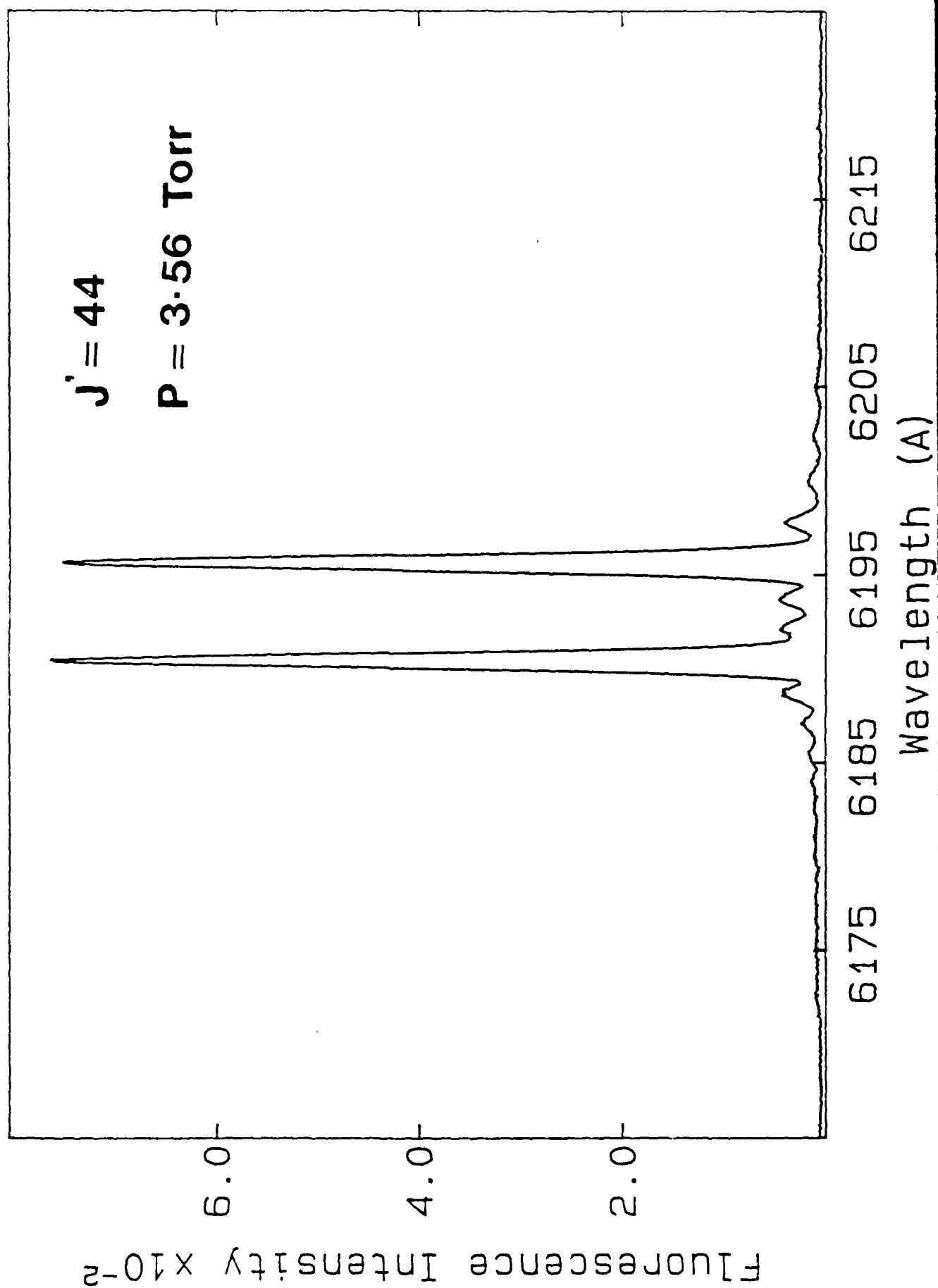


Figure 12.

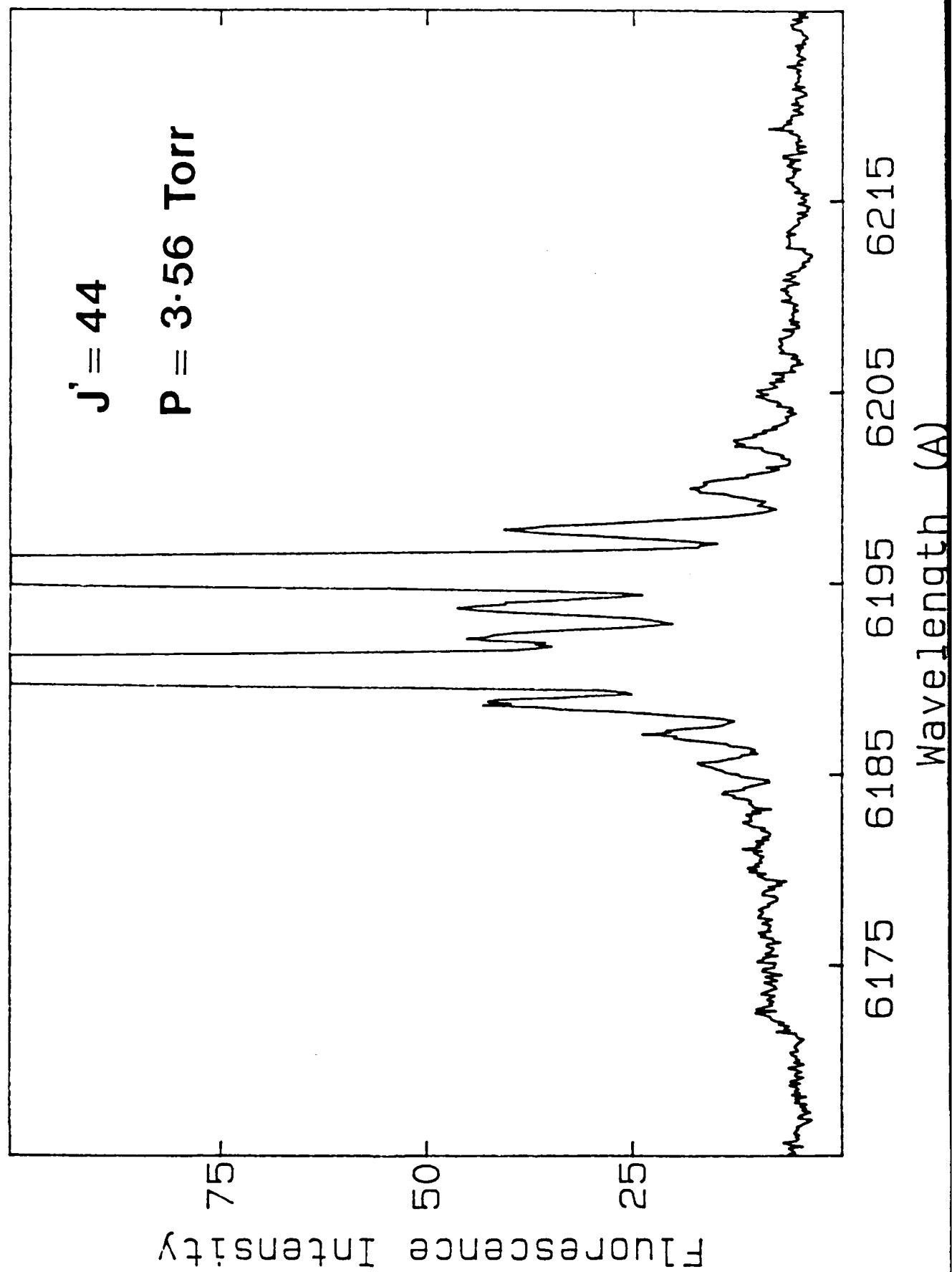


Figure 13.

Publications

1. L. J. van de Burgt and M. C. Heaven, Chem. Phys. 103, 407 (1986)
"Rate Constants for Collisional Deactivation of Br₂(B) by Br₂ (X) and He"
2. J. P. Nicolai and M. C. Heaven, J. Chem. Phys. 84, 6694 (1986)
"Electronic Quenching of I₂(B) by He at Low Collision Energies"
3. M. C. Heaven, Chem. Soc. Rev. 15, 405 (1986)
"Fluorescence Decay Dynamics of the Halogens and Interhalogens"
4. J. P. Nicolai and M. C. Heaven, J. Chem. Phys. 87, 3304 (1987)
"Emission Spectra for Matrix Isolated IF: Observation of New Low-Lying Electronic States"

Publications in preparation

1. L. J. van de Burgt and M. C. Heaven
"Radiative Lifetime Measurements for the B state of Chlorine Monofluoride"
2. W. Fawzy, M. Macler, J. P. Nicolai, and M. C. Heaven
"The Spectroscopy and Energy Transfer Dynamics of Matrix Isolated Iodine"

END

DATE

FILMED

5-88

DTIC